Infrared remote temperature measurements: its physics with reference to complexities, approximations and limitations involved. II—Temperature profile retrieval

RAJENDRA KUMAR GUPTA
Indian Institute of Tropical Meteorology, Pune 411 005

Received on December 20, 1977; Revised on March 13, 1978

Abstract

With a tentative inclination to complexity, approximation and limitation aspects the process of temperature profile determination in cloudless conditions, effect of '*a priori*' statistical constraint in improving the vertical resolution, reduction of retrieval problem into Fredholm linear integral equation of first kind and its solution using regression method, and comparison of retrieved profile with radiosonde-rocketsonde data have been discussed. Effect of spatially correlated errors and observation density towards limitations of satellite-based radiance measurements and the newly reported technique of channel differencing towards increasing vertical resolution of temperature measurements have been discussed. Methods of obtaining temperature profiles in the presence of clouds using single field and multiple field of views have been presented. The practices of accounting for geographical imposition of high terrain and the effect of hot terrain and a brief mention of effect of aerosols have been covered. A very short account of microwave remote temperature measurements, in order to attend to the efforts made in this direction, has also been included.

Key words: Infrared satellite temperature profile measurements, Clouds and remote temperature profile measurements.

1. Introduction

Kaplan[1] first expressed the possibility of exploiting the 15 μm CO_2 band for the passive remote measurement of atmospheric temperature profile. The uncertainties, approximations, and limitations of remote temperature estimation physics and lower boundary value estimation which effect the profile retrievals have been discussed by the author in Part I. In this part, the author will deal with the temperature profile estimation aspect. In retrieving profile information, the basic problem is of finding out a physical relationship relating uniquely the measured radiances with the desired parameter of interest, *i.e.*, a function $f(x)$, say temperature, is to be determined by measurement of another function $g(y)$, say radiance, while there exists no unique relationship between x and y. Since the basic methods which could be used in retrieving the atmospheric temperature and composition information from remote radiance measurements have been recently reviewed by Rodgers[2], the author does not wish to go into the details

of that aspect of the problem again but will only deal with one of the most commonly used method of temperature profile estimation in order to discuss the physical limitations involved. To deal with the realistic problem, retrieving of information in cloudy environment, the effects of high terrain, hot terrain and aerosols have been discussed. In the last the author has deviated from the main theme in submitting a very short account of microwave remote temperature measurements just to acknowledge the attempts made in this direction.

2. Determination of temperature profile in cloudless conditions

The radiative transfer equation for space-based passive remote sensing could be written as

$$I(\nu, 0) = B[\nu, T(x_0)]\,\tau(\nu, x_0, 0) - \int_0^{x_0} B[\nu, T(x)]\,\frac{d\tau(\nu, x, 0)}{dx}\,dx \qquad (1)$$

where $I(\nu, \theta)$ refers to observed radiance at an inclination θ to the vertical in channel corresponding to central frequency ν, $B[\nu, T(x_0)]$ and $\tau(\nu, x_0, \theta)$ refer to Planck black body function and transmission function corresponding to lower boundary radiation. x is a single valued function of pressure and the integration from 0 to x_0 covers the whole atmosphere from surface (x_0) to satellite level. $T(x_0)$ thus refers to surface temperature. Within the integral sign the $B[\nu, T(x)]$ and $d\tau(\nu, x, \theta)/dx$ are the Planck black body function and weighting function respectively. The first and second terms of eqn. (1) represent the radiation contributions from surface and intervening atmosphere respectively. The various physical approximations and limitations involved in arriving at the equation have been discussed by the author in Part I.

Radiance measurements are made in different channels of emission band. Different workers choosing different infrared spectral regions and different measurement techniques such as selective chopper radiometer (Houghton and Smith[3]; Barnett *et al.*[4]: Ellis *et al.*[5]) for lower levels and pressure modulator radiometer (Houghton[6]; Curtis *et al.*[7]) for upper levels have contributed to the measurement of temperature with satellite. In addition, the technique, of limb radiance measurements (Gille *et al.*[8]; Gille[9]) and various microwave region measurement techniques are being used by different workers. Based on limb scanning technique, the limb scanning pressure modulator radiometer (Rodgers[10]) and the limb scanning radiometer (Russel[11]) will be flown in Nimbus G scheduled for launch in 1978.

Besides being nonlinear, the retrieval problem is under constrained and it is difficult to find a unique solution profile from radiance measurements because of non-uniqueness in the observed radiance arising out of noise in physical measurements and due to ill-posed nature of the problem and for this reason the problem of extracting temperature profile from satellite radiance measurements is normally tackled as an estimation

problem by statistical and nonstatistical methods by putting direct or indirect constraints in order to get a solution profile whose error bounds are finite. Some arbitrary constraints, generally a minimization constraint, are used in nonstatistical methods. It may be mentioned here that even if $I(\nu, 0)$ is completely known as function of ν the integral eqn. (1) does not have an unique solution (Courant and Hilbert[12]). Putting a constraint is just to say something about the unknown profile and is usually equivalent to imposing a vertical resolution on the solution comparable to the width of weighting function and it could be done using statistical profile, forecast profile, Twomey-Tikhonove method, linear representation method and discretization method. The author proposes to discuss here the widely used regression method, where climatological or forecast profile is used as *a priori* constraint, for temperature profile retrieval from radiance measurements at discrete levels. The statistics which is based on radiosonde or rocketsonde data could be either regarded as a constraint or an extra set of observations of high resolution with a relatively high noise. Whether the inclusion of *a priori* statistics could improve the vertical resolution of remote temperature measurement has been discussed, on the basis of a numerical experiment, by Rodgers[13] using Backus and Gilbert[14] method. This method was originally developed for remote sounding of solid earth structure using seismic waves. It is a compromise between resolution and noise and refers to the estimation without *priori* information. As the statistical data used are available at discrete points the width of weighting function corresponding to these are taken to be equal to the spacing of the points. Rodgers[13] plotted trade-off diagrams between the spread (in scale height unit) and noise (in °K unit) to see whether the linear combination of weighting functions derived using Backus-Gilbert method could be made narrower, which in turn will improve the vertical resolution, as compared to original weighting functions by the inclusion of statistics. Assuming the ideal conditions for measurements, the trade-off diagrams were plotted for exclusive linear combination of weighting functions, for statistics only, and for a combination of both using algebra given in Conrath[15]. These trade-off diagrams were plotted for two situations simulating climatological statistics and the statistics of forecast error. The diagrams depict a substantial improvement in decreasing the spread by the inclusion of statistics justifying the use of '*a priori*' statistics as constraint.

Corresponding to the level of peak of weighting functions, Fig. 1 depicts the variation of $d\tau/dx$, where $x(p)\, ap^{2/7}$, with pressure in the window channel centering at $899{\cdot}0\ cm^{-1}$ and seven channels, centered at $750{\cdot}0\ cm^{-1}$, $734{\cdot}0\ cm^{-1}$, $709{\cdot}0\ cm^{-1}$, $701{\cdot}0$ cm^{-1}, $692{\cdot}0\ cm^{-1}$, $679{\cdot}8\ cm^{-1}$ and $668{\cdot}7\ cm^{-1}$, of 15 μm carbon dioxide band used in SIRS-B (Satellite Infrared Spectrometer-B) experiment. The technique of deriving temperature profile from measurements at discrete levels requires some modification to eqn. (1). Since in satellite experiments $I(\nu, 0)$ is measured only at discrete levels and the Planck function dependence on temperature is exponential a little error in the measurement of $I(\nu, 0)$ may lead to large errors in the determined value of temperature. Thus the estimation of temperature profile requires very accurate values of

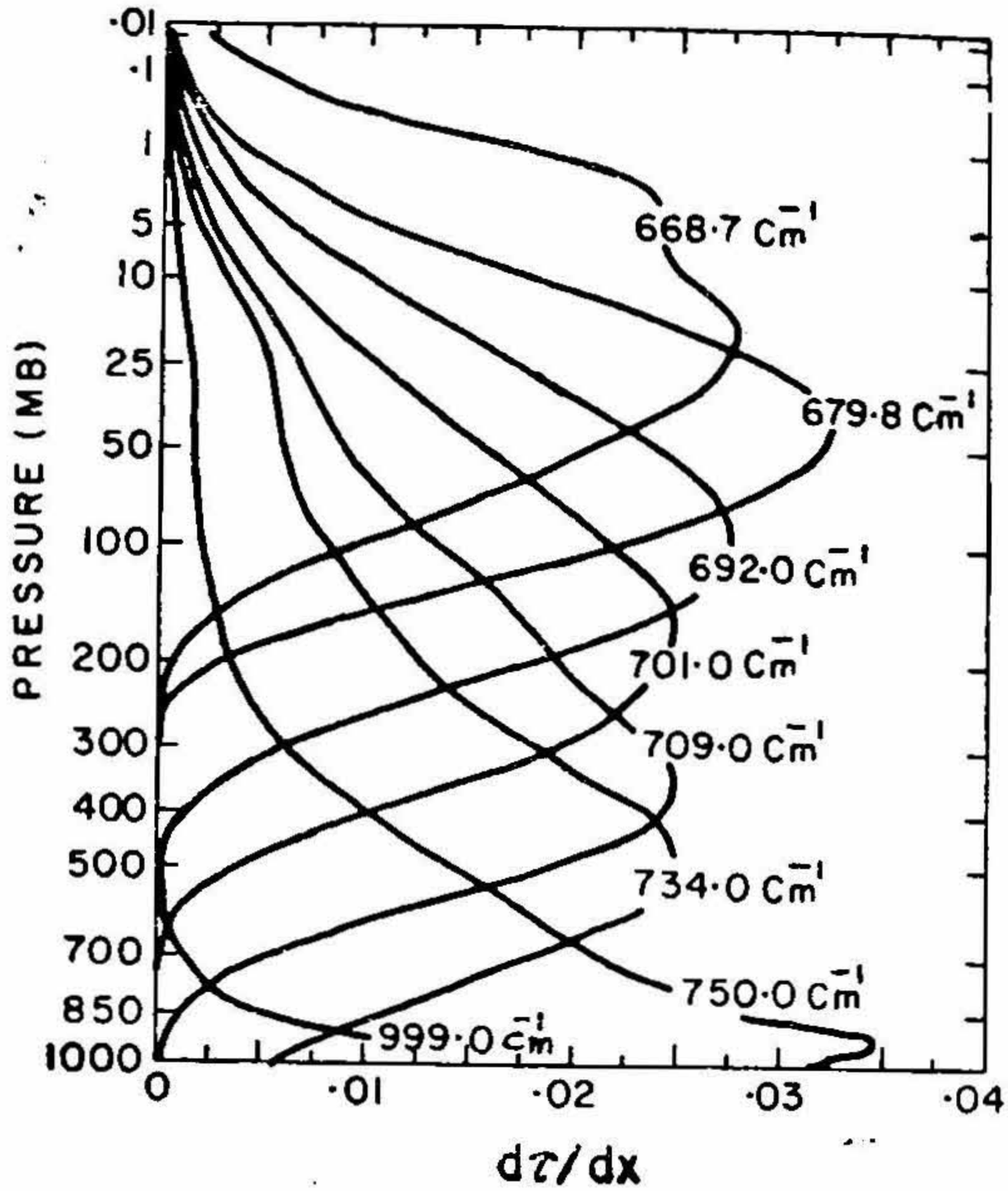

FIG. 1. Derivative of transmittance with respect to $x(p) \propto p^{2.17}$ (after Smith *et al.* [10]).

transmittance function, weighting function and surface temperature. Equation (1) could be rewritten as

$$\int_0^{x_0} B\,[\nu,\, T(x)]\, \frac{d\tau\,(\nu, x, 0)}{dx}\, dx = I\,(\nu, 0) - B\,[\nu,\, T(x_0)]\, \tau\,(\nu, x_0, 0). \tag{2}$$

On the right hand side of eqn. (2), $I(\nu, 0)$ is the radiance measured by satellite and the value for second term could be estimated from window channel measurements as discussed in Part I under the head 'measurement of surface temperature'. The integral on the left hand side of eqn. (2) has Planck function which is nonlinear both in frequency and temperature, the degree of dependency on ν (frequency or wave-number as it will involve only the change in the values of constants C_1 and C_2 of Planck function) in a narrow spectral interval in the infrared region being less as compared to that on the temperature 'T'. To reduce the eqn. (2) in the Fredholm linear integral equation of the first kind, the nonlinearity of $B\,[\nu, T(x)]$ in T needs to be approximated. Taking advantage of the conservative nature of the atmosphere, the magnitude of the problem of determining temperature profile $T(x)$ could be reduced to the problem of determining deviations from climatic profile $\bar{T}(x)$ (or from the

forecast profile, if available) which becomes necessary in order to approximate Planck function nonlinearity in T in linear form. Defining

$$h(x) = T(x) - \bar{T}(x) \tag{3}$$

as the deviation of the actual profile from climatic profile, the Planck function $B[\nu, T(x)]$ could be approximated by expanding it about a reference profile $\bar{T}(x)$ as shown in eqn. (4)

$$B[\nu, T(x)] = B[\nu, \bar{T}(x)] + \frac{dB[\nu, \bar{T}(x)]}{dT}[T(x) - \bar{T}(x)]$$

$$+ \text{terms of higher orders.} \tag{4}$$

Retaining only first two terms on the right hand side of eqn. (4) towards a linear approximation of Planck function $B[\nu, T(x)]$ and substituting this to eqn. (2), we get

$$\int_0^{z_0} \frac{dB[\nu, \bar{T}(x)]}{dT} \frac{d\tau(\nu, x, 0)}{dx} h(x)\, dx$$

$$= I(\nu, 0) - B[\nu, T(x_0)]\, \tau(\nu, x_0, 0) - \int_0^{z_0} B[\nu, \bar{T}(x)] \frac{d\tau(\nu, x, 0)}{dx} dx. \tag{5}$$

The third term on the right hand side of eqn. (5) could also be estimated using climatic temperature profile thus reducing the whole of the right hand side to a known quantity

$$r(\nu, 0) = I(\nu, 0) - B[\nu, T(x_0)]\, \tau(\nu, x_0, 0)$$

$$- \int_0^{z_0} B[\nu, \bar{T}(x)] \frac{d\tau(\nu, x, 0)}{dx} dx. \tag{6}$$

The first two terms on the left hand side of eqn. (5) could be written as

$$k(\nu, x) = \frac{dB[\nu, \bar{T}(x)]}{dT} \frac{d\tau(\nu, x, 0)}{dx} \tag{7}$$

where $K(\nu, x)$ is known as the kernal function. Thus under the notations mentioned in eqns. (6) and (7) the eqn. (5) reduces to

$$\int_0^{z_0} k[\nu, x]\, h(x)\, dx = r(\nu, 0). \tag{8}$$

Equation (8) is a Fredholm linear integral equation of the first kind having $r(\nu, 0)$ values available at discrete levels and the kernal function in tabular form. This equa-

tion is difficult to be solved by analytical methods and is thus solved by numerical methods. The numerical solving of eqn. (8) using power polynomials is preferred over the use of trignometric-, rational-, exponential-, hyperbolic-, and logarithmic functions for the reason that differentiation and integration of power polynomials will not give rise to different functions and will simply change the degree of the polynomial and the value of the coefficients. According to Weierstrass's theorem any arbitrary continuous function, irrespective of its pathology, in a finite interval could always be approximated over the whole range of interval as closely as desired by a power polynomial of sufficiently high degree. The integral is approximated using quadrature techniques by dividing the integration interval into $(N + 1)$ intervals which may or may not be equally spaced. Thus eqn. (8) using quadrature method (Fritz *et al.*[16]) could be reduced to

$$r_i = \sum_{j=1}^{N} \omega_j k\,(v_i, x_j)\, h_j \triangle x_j \tag{9}$$

where ω_j are the quadrature weights for particular values of function $h(x_j)$, briefly h_j, with abscissae x_j. Here $j = 1, 2, 3, \ldots, N$ and $i = 1, 2, 3, \ldots, M$, M being the number of levels from which satellite receives the radiance. Putting $a_{ij} = \omega_j\, k\,(v_j, x_j)\, \triangle x_j$ eqn. (9) reduces to

$$r_i = \sum_{j=1}^{N} a_{ij} h_j$$

or $[r] = [A]\,[h]$ in matrix notation.

The nature of a_{ij} is mainly determined from the weighting functions which occur in the overlapping form resulting in the ill-conditioning of matrix $[A]$ for inversion making direct solution for $[h]$ impracticable. The near linear dependence of its adjacent rows and columns results in the ill-conditioning of matrix $[A]$ for inversion making direct solution for $[h]$ impracticable as the solution 'h' does not depend continuously on the data function 'r'. Due to continuous nature of integral operator $[A]$ which may contain a cluster of small eigenvalues the attempt to solve the system directly may lead to wildly oscillating solutions (Miller[17]). It may be noted that in equation (8) only those matching values of $r\,(v, 0)$ which lie in the range of $k\,(v, x)$ will be taken care of and also the kernal function $k\,(v, x)$ smoothes out, the degree of which depends on the kernals' nature, the roughness and discontinuities of $h\,(x)$. Miller[17] has overviewed the subject of Fredholm integral equations of first kind, a problem of much academic interest and mathematical elegance which has been dealt with by Twomey[18], Strand and Westwater[19, 20], Westwater and Strand[21], Wahba[22], Strand[23] and many other workers of which a brief account also occurs in Colin[24].

Regression method of analysis

As discussed in Part I there are enough approximations involved in the formulation of weighting and transmittance functions besides the difficulties relating to calibration and measurement biases and under such circumstances the regression method of

extracting temperature profile from radiance measurements at discrete levels becomes very useful as compared to inverse matrix and direct methods. The derivation of temperature profile from measurements of radiance at discrete levels is physically based on the following reasonings:

(i) Due to the shape and overlapping of weighting functions the radiance received in a particular interval will have radiance contribution from other levels in addition to the main radiance contribution corresponding to the level where the particular weighting function has its peak. Thus the information about temperature of other levels is also present in the radiance measured in a particular interval.

(ii) Since any one level in the atmosphere is physically as well as radiatively linked with other distant levels in the atmosphere there will also be reflection of temperature of other levels in the measurement of radiance in a particular interval.

Due to above cited reasoning the temperature at a particular level could be statistically related to radiances measured in all the spectral intervals (Fritz *et al.*[16]). To utilize this concept towards the formulation of a transfer matrix for generating profile of $h(x)$ out of measurements of radiance r_i ($i = 1, 2, 3, \ldots M$) following information is to be gathered.

(i) Satellite radiance measurement r_i for M levels, *i.e.*, $i = 1, 2, 3, \ldots, M$.

(ii) Radiosonde and rocketsonde measurements, coincident in space and time, say for N levels. Here the encountered problems of geographical registration and objective interpolation will be affecting the accuracy of the method.

Taking a large number of pairs of such data, say L, we can define a matrix for $h(x)$ and $r(v, \theta)$ as

$$H = [h_{jk}], j = 1, 2, 3, \ldots, N;\ k = 1, 2, 3, \ldots L.$$

and

$$R = [r_{ik}]\ i = 1, 2, 3, \ldots, M;\ k = 1, 2, 3, \ldots L.$$

Let $C = [c_{ji}]$ be the transformation matrix such that $H = CR$. The matrix C is estimated in the least square sense by minimizing the Euclidean distance

$$\mathcal{E}(C) = \sum_{j,k=1}^{N,L} \left(h_{jk} - \sum_{i=1}^{M} C_{ji} r_{ik}\right)^2. \tag{10}$$

Equation (10) could also be written as

$$\mathcal{E}(C) = \text{Trace}\,[(H - CR)(H - CR)^T].$$

Applying condition $\frac{d\mathcal{E}(C)}{dC} = 0$, one gets (11)

$$C = HR^T (RR^T)^{-1}.$$

The transformation matrix arrived in this way using data of a zone will be valid for that zone only and over the ocean for the reasons of paucity of conventional data it leaves scope for continuous editing with more and more data. For $(RR^T)^{-1}$ to exist (RR^T) should not be a singular matrix, *i.e.*, the determinant of (RR^T) should not vanish which in turn requires that L should be much larger than M. Once the transformation matrix for a particular place is determined the $h(x)$ profile can be calculated using observed radiance measurements.

Since

$$h(x) = T(x) - \bar{T}(x)$$

$$T(x) = \bar{T}(x) + h(x).$$

Thus knowing $h(x)$ and adding it to already used climatic profile $\bar{T}(x)$ will give the desired temperature profile. The use of forecast profile in place of climatic profile will improve the estimate.

It is necessary to mention here that satellite temperature measurements are over a wide area while radiosonde measurements are along specific trajectory and thus it is natural to encounter random errors while comparing retrieved temperature profiles with nearly coincident radiosonde profiles. However, trends are often found in these random discrepancies which could be due to systematic errors in measurements, in calibration, in retrieval procedure, in estimated atmospheric transmittance values, and also due to inherent limitations in accounting for the effects of clouds (discussed later). Jastrow and Halem[25] and Wark[26] considering the cause for these trends in the atmospheric transmittance estimation errors attempted the problem by empirically adjusting the atmospheric transmittance values and have achieved limited success. As the systematic errors could arise due to various reasons, Weinreb and Fleming[27] attempted the problem by doing empirical adjustments to clear column radiances and found that their method combined with the method of transmittance adjustments could result in better improvement of temperature profile derived from Vertical Temperature Profile Radiometer (VTPR) measurements. They conclude that radiance adjustments are more effective than transmittance adjustments in improving retrieved profiles though radiance adjustments alone were not able to effect much improvement. The vertical resolution of retrieved temperature profile could be improved by decreasing the width of the weighting function. Recently Fleming[28] has discussed the reduction of this width by the process of channel differencing. In the radiative transfer equation the radiance received at satellite (I) after its scaling to a fixed reference wave number could be written as

$$\tilde{I}_i = B_r[T(x_0)]\,\tau_i(x_0) - \int_0^{x_0} B_r[T(x)]\,\frac{d\tau_i(x)}{dx}\,dx$$

where suffix $i = 1, 2, \ldots, N$ refers to spectral intervals. Integrating the above equation by parts one gets

$$\tilde{I}_i = B_r[0] + \int_0^{z_0} \frac{dB_r[T(x)]}{dx} \tau_i(x)\, dx$$

as $\tau_i(0) = 1$. In this equation the lower boundary term has disappeared. Now say for two channels $i = 2j + 1$ and $i = 2j$, the difference of scaled radiance will be

$$\tilde{I}_{2j+1} - \tilde{I}_{2j} = \int_0^{z_0} [\tau_{2j+1}(x) - \tau_{2j}(x)] \frac{dB_r[T(x)]}{dx}\, dx$$

or

$$\triangle I_j = \int_0^{z_0} K_j(x)\, g(x)\, dx$$

where

$$\triangle I_j = \tilde{I}_{2j+1} - \tilde{I}_j;\ K_j(x) = [\tau_{2j+1}(x) - \tau_{2j}(x)]$$

and

$$g(x) = \frac{dB_r[T(x)]}{dx}$$

$\triangle I_j$ could be experimentally obtained by chopping between pairs of channels. The channel differencing method reduces the weighting function width by 20%, does not involve surface boundary term and removes the systematic errors by virtue of differencing operation. The equation describing $\triangle I_{ij}$ could be solved for $g(x)$ and in turn for Planck function profile by integration method from which temperature profile could be derived. Fleming has also discussed the matrix method and has compared, undertaking simulation studies, these two types of solutions involving channel differencing with the information derived without channel differencing by minimum information solution. He has studied the RMS error of these methods for levels from 1000 mb to 10 mb. The RMS error of solutions involving channel differencing method was consistently higher than that of minimum information solution. The cause for such negative result could be traced in the decreased signal to noise ratio due to differencing operation and further in the increase of RMS value of random noise by $\sqrt{2}$ factor in differenced radiance as compared to individual radiance. Among the two solutions for channel differencing the matrix solution was consistently better than the integral method because in the latter method integration of derivative solution $f(x)$ $= dB/dx$ needs constant of integration which is assigned by *a priori* temperature at one point in the atmosphere and the error in it will propagate throughout the entire profile. Additionally the integration process will smoothen the random noise in solu-

tion profile and also the realistic fine structure in temperature profile. In matrix solution, matrix for differencing case has been more ill-conditioned as compared to that for non-differencing case. The differencing approach, though principally could give better vertical resolution, is not able to contribute due to limitations involved in solution and reduced signal to noise ratio.

Prabhakara *et al.*[29] have analysed the Nimbus 4 IRIS data for the period from April 1970 to January 1971 and have discussed the stratospheric thermal structure. Examining mean global distribution of satellite-derived stratospheric temperatures for April, July, October and December 1970, they found that though large scale features in temperature field alongwith their seasonal variations could be more or less reproduced, the sharp temperature minimum near 100 mb over tropical latitudes could not be reproduced. They further found that both radiosonde and satellite measurements have shown nearly isothermal structure between 100 and 30 mb levels over high latitudes during winter and spring. An excess of estimation by 10° K over tropical latitudes and lower values at 100 mb level and higher values at 10 mb level over high latitudes (Northern Hemisphere) were observed when retrieved temperatures were compared with radiosonde observations. Besides the errors arising out of objective procedure for specifying the initial guess of temperature profile, the errors in the calibration procedure could contribute to some extent for the observed systematic errors. The northeast to southwest tilt in northern hemisphere and northwest to southeast tilt in southern hemisphere in the ridges and troughs of the standing waves on constant pressure surfaces, necessary for poleward transport of heat, were observed in satellite temperature maps. They found that the position and tilt of standing waves and their westward slope with height while going upward from 100 to 10 mb level had reasonable agreement with climatology. They further observed that the diminishing of amplitude of large scale standing waves with height in between 100 and 10 mb levels in the middle and high latitudes was found to be more rapid than what could be suggested by climatology. Recently Horn *et al.*[30] have also intercompared the data derived from satellite radiance measurements with rawinsonde observations and initialized Limited Area Fine Mesh (LFM) model fields.

The Global Atmospheric Research Program (GARP[31]) has laid down the $\pm$ 1° C and 500 km as the resolution requirements for temperature measurements. Satellite-based temperature measurements are unable to provide the specified accuracy of $\pm$ 1° C and it is argued that the enormous coverage provided by satellite-based temperature measurements will be able to compensate the accuracy limitation. Unlike radiosonde observations where errors used to be random and mutually independent, systematic errors due to the presence of large scale cloud patterns could get reflected in the satellite-derived temperature soundings. Following Gandin[32] approach in formulating equation for spatially correlated and unbiased measurement errors and extending Alaka and Elvander[33, 34] method to include the effects of spatially correlated errors, Bergman and Bonner[35] numerically studied the effects of spatially correlated errors and of observation density on the error of analysis for analysis point located

at the centre of a 12-point rectangular grid. For the sake of understanding the limitations of satellite-based temperature measurements it is proposed to present a view of this paper. Bengtsson and Gustavsson[36] studying the spatial correlation of 12-hour forecast errors of 500 mb geopotential height fitted the following analytical expression to the spatial correlation *versus* the observational spacing curve

$$\mu_{ij}(s) = \exp(-k_\mu S^2)$$

where μ_{ij} is the spatial correlation between the ith and jth points in space separated by a distance 'S' in k_μ and is equal to $1{\cdot}56 \times 10^{-6}$ km^2. Bergman and Bonner assumed the validity of this functional relationship with the same value for k_μ for the spatial correlation of 12-hour forecast temperature errors. Comparing Nimbus 5 temperature profile data obtained by statistical regression method with three hand-drawn cross-sections based on radiosonde data representing three synoptic situations, Bergman and Bonner arrived at the following analytical expression towards spatial correlations for Nimbus 5 satellite observational errors for temperature

$$\rho_{ij} = \exp(-8k_\mu S^2).$$

Considering this observation they modelled the spatial correlation error ρ_{ij} as

$$\rho_{ij} = \exp(-k_\rho S^2)$$

where k_ρ assumed values equal to k_μ, $8k_\mu$ and infinity. Assuming $k_\rho = k_\mu$ means same spatial correlation value for satellite temperature error and forecast error (may be applicable to the data retrieval case where forecast profile is used as a constraint). Assuming $k_\rho = 8k_\mu$ and $k_\rho = \infty$ mean the spatial correlation observed in Nimbus 5 data using rawinsonde analysis, no spatial correlation of observational errors respectively. The effect of observational density was studied by varying the spacings in between the grid points for 100 to 1,600 km. Figs. 2, 3, and 4 depict the variation of normalised analysis error (σ_a) as a function of 'h', the distance between the grid points in km, with three model values of k_ρ for the three cases corresponding to $\sigma_\epsilon = 0{\cdot}25$, $0{\cdot}5$ and $1{\cdot}0$, σ_ϵ being the normalised observational error. In all these figures the curve 'A', plotted for $\sigma_\epsilon = 0$ corresponding to perfect observation case, depicts that component of analysis error which arises due to the spatial interpolation of the observations to the grid point. Curves marked 'B' in these figures represent the case of random independent errors while the curves marked 'C' and 'D' depict the cases of spatially correlated errors. From curves marked 'A' it could be inferred that analysis error resulting from spatial interpolation of observations is negligible for $h < 400$ km. The curves show that the magnitude of analysis error is more for $k_\rho = k_\mu$ than for $k_\rho = 8k_\mu$ as the former represents higher degree of spatial correlation. The analysis error for $k_\rho = \infty$ representing spatially independent observation is less as compared to that for spatially correlated errors. It could further be seen that spatial interpolation contribution to analysis error is much for widely spaced observations while for closely spaced observations the primary contribution to analysis error is from the

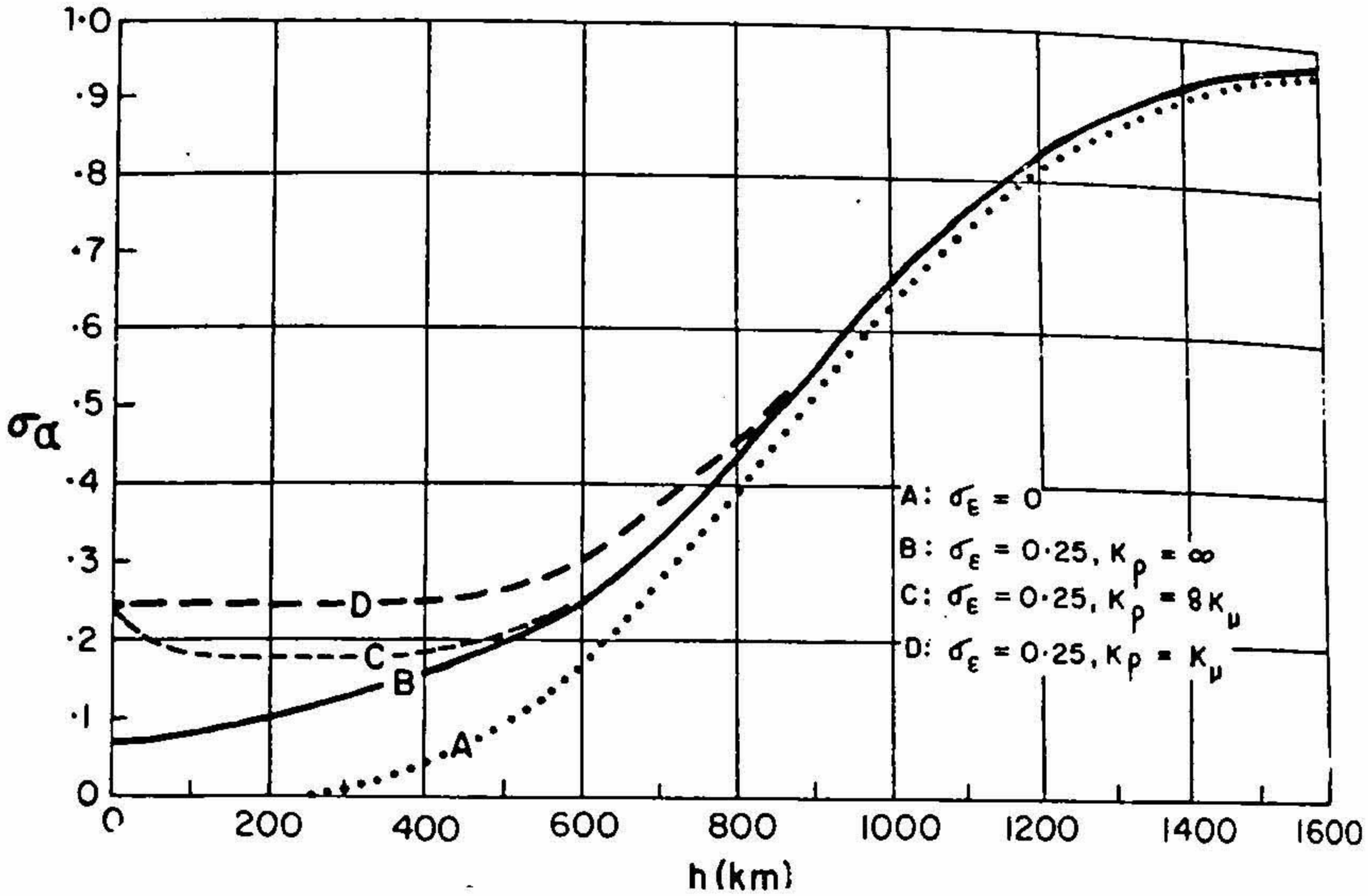

FIG. 2. Normalized standard deviation analysis error σ_a as a function of observational spacing h for $\sigma_\epsilon = 0$ and for three cases where $\sigma_\epsilon = 0{\cdot}25$. The curve $k\rho = \infty$ applies to uncorrelated observational errors (after Bergman and Bonner[35]).

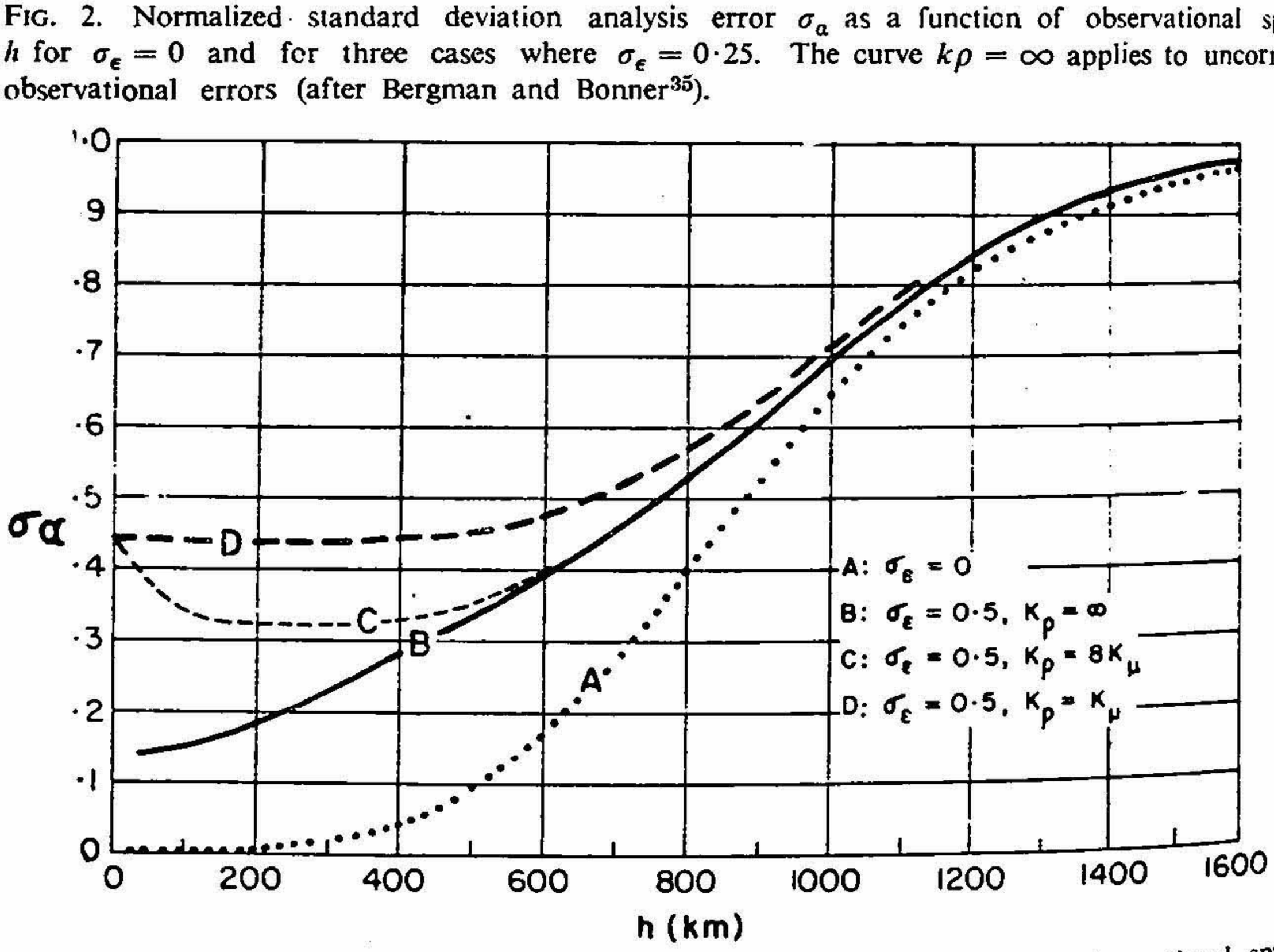

FIG. 3. Normalized standard deviation of analysis error σ_a as a function of observational spacing h for $\sigma_\epsilon = 0$ and for the cases where $\sigma_\epsilon = 0{\cdot}5$. The curve $k\rho = \infty$ applies to uncorrelated observational errors (after Bergman and Bonner[35]).

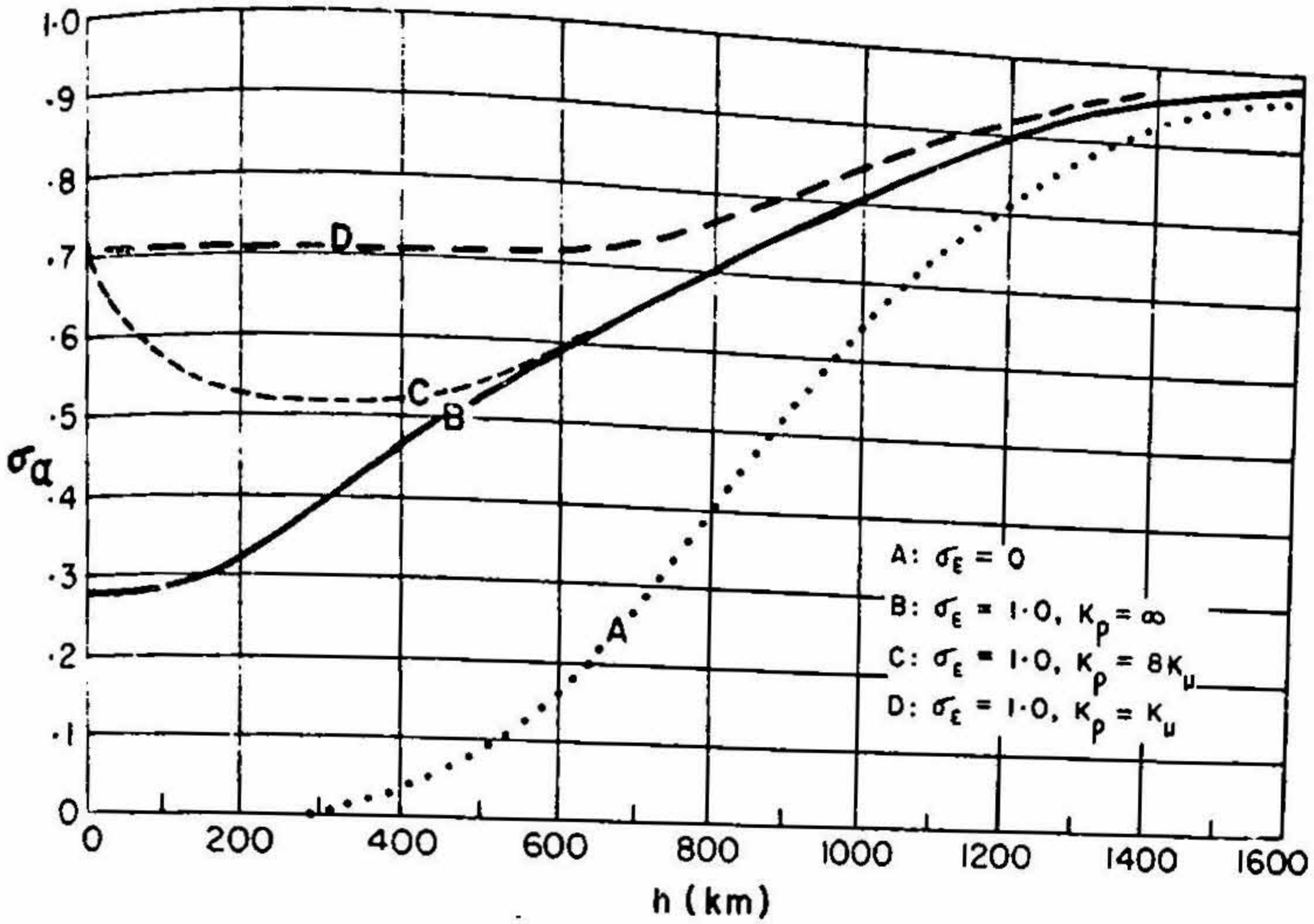

FIG. 4. Normalized standard deviation of analysis error σ_a as a function of observational spacing h for $\sigma_\epsilon = 0$ and for the cases where $\sigma_\epsilon = 1{\cdot}00$. The curve for $k\rho = \infty$ applies to uncorrelated observational errors (after Bergman and Bonner[35]).

observational errors. Bergman and Bonner conclude that increasing the density of observations beyond a spacing of 400 km will not yield any substantial improvement in the temperature analysis which uses satellite-based measurements. Gandin *et al.*[37] also carried out similar studies for geopotential height using a triangular observation network having observations at its vertices and the analysis point at its centre. Referring to Gandin *et al.*, Bergman and Bonner[38] also conclude, as Gandin *et al.* have concluded, that in order to get information content comparable to that of rawinsonde the observational errors for satellite-based measurements should be smaller.,

3. Methods of solution for profile determination in the presence of clouds

(*a*) *General considerations*

Presence of clouds in the field of view creates complexity because clouds absorb infrared radiations. The opaqueness of cloud depends upon the droplet spectrum, ice particle distribution (if ice phase is present) and saturated water vapour characteristics inside the clouds while the cloud contribution to the observed radiance depends on the cloud structure and top surface characteristics which involve water drops, ice and saturated water vapour as these will be responsible for emission from the cloud top. Since clouds beside being of different microphysical and dynamical structures possess

different vertical extent to horizontal extent ratios with tops emerging at different altitudes the problem of determining opacity of cloud to radiations emerging from atmosphere below cloud bottom including earth surface becomes a tedious job. Similarly the determination of emissivity of cloud top is also a difficult problem. Inclusion of all these characteristics in the analysis will mean involving more unknown parameters than the number of independent information available from present day measurements with satellite. Based on the experimental study of the transfer of infrared radiation through stratus clouds, Kuhn *et al.*[39] developed a simple model for transfer of infrared radiations through clouds. Besides the lack of proper understanding of infrared radiative transfer through clouds, the presence of different types of clouds as discussed earlier forbids the use of physical inputs including modifications and perturbations from clouds in the radiative transfer equation formulation. Two basic techniques, *viz.*, single field of view and multiple field of view for finding out clear column radiance $[I_{clr}(v, \theta)]$ from radiance measurements $[I(v, \theta)]$ by satellite in the presence of clouds have been discussed by Smith *et al.*[40] and Fritz *et al.*[16] Both the techniques are mainly based on the consideration that atmosphere used to consist of broken clouds.

Using a high spatial resolution radiometer/spectrometer it is possible to get the radiances either from cloud regions $[I_{cd}(v, \theta)]$ or clear regions $[\bar{I}_{clr}(v, \theta)]$ and this is the physical basis of single field of view approach. Here the most probable value of $I_{clr}(v, \theta)$ is achieved treating the observed radiances as an ensemble of $I_{clr}(v, \theta)$ and $I_{cd}(v, \theta)$. If there are n number of cloudy columns and m number of clear columns then

$$N = \frac{n}{n + m}$$

will represent the relative amount of cloudiness and if $\bar{I}(v, \theta)$ is the average radiance received by satellite over $(n + m)$ columns then

$$\bar{I}(v, 0) = \frac{1}{n + m}\left[\sum_{i=1}^{n} I_{cd}^{i}(v, 0) + \sum_{i=1}^{m} I_{clr}^{i}(v, 0)\right] \tag{12}$$

Defining by $\bar{I}_{cd}(v, 0)$ and $\bar{I}_{clr}(v, 0)$ by

$$\bar{I}_{cd}(v, 0) = \frac{1}{n}\sum_{i=1}^{n} I_{cd}^{i}(v, 0)$$

and

$$\bar{I}_{clr}(v, 0) = \frac{1}{m}\sum_{i=1}^{m} I_{clr}^{i}(v, 0)$$

respectively, substituting for the terms on the right hand side of eqn. (12) and deleting the average sign, we get

$$I(\nu, 0) = NI_{cd}(\nu, 0) + (1 - N) I_{clr}(\nu, 0). \tag{13}$$

Knowing $I_{cd}(\nu, 0)$ and N, $I(\nu, 0)$ being known, $I_{clr}(\nu, 0)$ could be estimated. Equation (13) could be interpreted to represent the observed radiance in a low resolution instrument where N is the effective fractional field of view covered by clouds. Two approaches, *i.e.*, assuming all the clouds distributed either in a single layer or in a double layer could be used in a simple manner, the latter one has been in use.

(b) Single layer approach

The radiance received at satellite in the presence of a single layer of cloud will have four components, *viz.*,

(i) The radiance emitted from the cloud, *i.e.*,

$$\varepsilon_c(\nu, 0)\, B[\nu, T(p_c)]\, \tau(\nu, p_c, 0),\ \varepsilon_c$$

being the emissivity of cloud

(ii) the radiance emitted from the levels above the cloud level, *i.e.*,

$$\int_{p_c}^{0} \varepsilon_c(\nu, 0)\, B[\nu, T(p)] \frac{d\tau(\nu, p, 0)}{dp}\, dp$$

(iii) the downward component of radiance having solar origin reflected by cloud layer, *i.e.*,

$$r_c(\nu, 0)\, I_d(\nu, p_c, 0)\, \tau(\nu, p_c, 0)$$

r_c and I_d being the reflectivity of cloud and reflected radiation.

(iv) The amount of upward component of the radiance at the cloud base transmitted by the cloud, *i.e.*,

$$t_c(\nu, 0)\, I(\nu, p_0, p_c, 0)\, \tau(\nu, p_c, 0)$$

t_c, being the transmissivity of cloud.

Since the reflectivity of cloud in 15 μm band is zero,

$$t_c(\nu, 0) = 1 - \varepsilon_c(\nu, 0). \tag{14}$$

Thus

$$I_{cd}(\nu, 0) = \varepsilon_c(\nu, 0) \left\{ B[\nu, T(p_c)]\, \tau(\nu, p_c, 0) - \int_0^{p_c} B[\nu, T(p)] \frac{d\tau(\nu, p, 0)}{dp}\, dp \right.$$

$$+ [1 - \varepsilon_e (\nu, 0)] I_{clr} (\nu, 0)$$
$$= \varepsilon_e (\nu, 0) I_{bc} (\nu, 0) + [1 - \varepsilon_e (\nu, 0)] I_{clr} (\nu, 0) \quad (15)$$

where

$$I_{bo} (\nu, 0) = B [\nu, T (p_c)] \tau (\nu, p_c, \theta) - \int_0^{p_0} B [\nu, T (p)] \frac{d\tau (\nu, p, 0)}{dp} dp$$

is the amount of radiance the cloud would have emitted had it been a black body.

Substituting for $I_{cd} (\nu, 0)$ in eqn. (13), we get

$$I (\nu, 0) = I_{clr} (\nu, 0) - \alpha [I_{clr} (\nu, 0) - I_{bo} (\nu, \theta)] \quad (16)$$

where $\alpha = N\varepsilon_e (\nu, 0)$ is the effective cloud amount.

or

$$I (\nu, 0) = B [\nu, T (p_0)] \tau (\nu, p_0, 0) - \int_0^{p_0} B [\nu, T (p)] \frac{d\tau (\nu, p, 0)}{dp} dp$$

$$- \alpha \left\{ B [\nu, T (p_0)] \tau (\nu, p_0, 0) - B [\nu, T (p_c)] \tau (\nu, p_c, 0) \right.$$
$$\left. - \int_{p_c}^{p_0} B [\nu, T (p)] \frac{d\tau (\nu, p, 0)}{dp} dp \right\} \quad (17)$$

or

$$I_{clr} (\nu, 0) = I (\nu, 0) + \alpha (\nu) Q (\nu, p_c) \quad (18)$$

where the first two terms on the right hand side of eqn. (17) correspond to $I_{clr} (\nu, 0)$ while the term within the brackets correspond to $Q (\nu, p_c)$, *i.e.*,

$$Q (\nu, p_c) = B [\nu, T (p_0)] \tau (\nu, p_0, 0) - B [\nu, T (p_c)] \tau (\nu, p_c, 0)$$
$$- \int_{p_0}^{p_0} B [\nu, T (p)] \frac{d\tau (\nu, p, 0)}{dp} dp$$

Since p_c represents the pressure at effective cloud level and α represents the effective cloud amount in a single layer while clouds in fact exist at several levels and further $\varepsilon_e (\nu, \theta)$ which appears in α itself varies with cloud nature, the eqn. (18) is a nonlinear equation in p_c and α. Determination of $I_{clr} (\nu, 0)$ using eqn. (18) will demand for the value of $\alpha (\nu)$ and $Q (\nu, p_c)$. Using cloud picture information one may be able to have an estimate of N but the estimate of $\varepsilon_e (\nu, 0)$ towards determining $\alpha (\nu)$ will be a problem.

Determination of $Q(\nu, p_e)$ needs the value of p_e and the temperature profile between levels p_e and p_0. Though cloud top pressures using high resolution infrared window data could be estimated, the estimation of effective value of p_e is a more difficult process. Taking radiance data from window channel (899 cm^{-1}) and five 15 μm band carbon dioxide channels which are most opaque to clouds (say 669·3, 677·8, 692·3, 699·3 and 706·3 cm^{-1}), the initial estimate of temperature profile using regression method discussed earlier could be deduced. Here it may be mentioned that using these channels, although the information input would be mostly from the levels at cloud level and above, the temperature profile below cloud level may be estimated on the assumption that it will be statistically related to temperatures at and above the cloud level. This first estimate is further improved by the method of iteration. For further improvement, two frequencies (central frequencies of the spectral intervals) which are most sensitive to clouds (say 714 cm^{-1}, 750 cm^{-1}) are used to determine p_e. Labelling these two frequencies by ν_1 and ν_2 eqn. (18) could be written for each as follows:

$$I_{clr}(\nu_1, 0) = I(\nu_1, 0) + a(\nu_1)\, Q(\nu_1, p_e)$$

$$I_{clr}(\nu_2, 0) = I(\nu_2, 0) + a(\nu_2)\, Q(\nu_2, p_e)$$

here

$$a(\nu_1) = N\varepsilon_e(\nu_1, 0) \quad \text{and} \quad a(\nu_2) = N\varepsilon_e(\nu_2, 0)$$

assuming that ε_e is same for ν_1 and ν_2 (N is the same since the field of view is also the same), above equations could be rewritten as $[a(\nu_1) = a(\nu_2) = a(\nu)]$

$$I_{clr}(\nu_1, 0) = I(\nu_1, 0) + a(\nu)\, Q(\nu_1, p_e) \tag{19}$$

$$I_{clr}(\nu_2, 0) = I(\nu_2, 0) + a(\nu)\, Q(\nu_2, p_e). \tag{20}$$

In order to eliminate $a(\nu)$ eqn. (20) is multiplied by $Q(\nu_1, p_e)$ and eqn. (19) is multiplied by $Q(\nu_2, p_e)$ and then on subtracting eqn. (20) from eqn. (19) we get

$$\{I_{clr}(\nu_1, 0) - I(\nu_1, 0)\}\, Q(\nu_2, p_e) - \{I_{clr}(\nu_2, \theta) - I(\nu_2, \theta)\}\, Q(\nu_1, p_e) = 0. \tag{21}$$

Since $I(\nu_1, \theta)$ and $I(\nu_2, 0)$ are known quantities, $I_{clr}(\nu_1, \theta)$ and $I_{clr}(\nu_2, \theta)$ could be estimated using first estimate of temperature profile and since in $Q(\nu_1, p_e)$ and $Q(\nu_2, p_e)$ all other parameters except p_e are known the above equation could be solved for the determination of p_e. Once first approximate value of p_e is estimated, corrected estimates of $I_{clr}(\nu, 0)$ could be obtained using this p_e value and first estimated profile, for those five opaque and window channels. Again by regression method second estimate of temperature profile is obtained and the process is repeated. This process of iteration is continued till the convergence, rather asymptotic nature, gets reflected and these values of $I_{clr}(\nu, 0)$ are considered to be the most probable values and finally the temperature profile is obtained using computed radiances for all the eight channels in the regression method.

(c) Two layer model

Here the distribution of clouds is assumed to exist at two levels and clouds at one level are considered to be distributed at random with respect to clouds at the other level meaning that breaks in the clouds in two layers are not correlated. Rearranging eqn. (16) we get

$$\{I(\nu, \theta)\}_L = a\{I_{bo}(\nu, \theta)\}_L + (1 - a) I_{clr}(\nu, \theta) \tag{22}$$

where subscript L to the braces refers to lower layer of the cloud. In case of upper layer of cloud $\{I(\nu, 0)\}_L$ will serve as clear column radiance and if β is the effective cloud amount for the upper layer then

$$I(\nu, \theta) = \beta\{I_{bo}(\nu, 0)\}_U + (1 - \beta)\{I(\nu, 0)\}_L \tag{23}$$

where subscript u to the braces refers to upper layer of cloud.

Substituting for $\{I(\nu, \theta)\}$ from eqn. (22) in eqn. (23) we get

$$I(\nu, \theta) = \beta\{I_{bo}(\nu, 0)\}_U + (1 - \beta)[a\{I_{bo}(\nu, 0)\}_L + (1 - a) I_{clr}(\nu, \theta)]$$

or

$$I(\nu, 0) = B[\nu, T(p_0)]\,\tau(\nu, p_0, 0) - \int_0^{p_0} B[\nu, T(p)]\,\frac{d\tau(\nu, p, \theta)}{dp}\,dp$$

$$-\beta\left\{B[\nu, T(p_0)]\,\tau(\nu, p_0, \theta) - B[(\nu, T(p_\mu)]\,\tau(\nu, p_U, \theta)\right.$$

$$\left.-\int_{p_U}^{p_0} B[\nu, T(p)]\,\frac{d\tau(\nu, p, 0)}{dp}\,dp\right\} - a(1 - \beta)\left\{B[\nu, T(p_\mu)]\,\tau(\nu, p_0, 0)\right.$$

$$\left.-B[\nu, T(p_L)]\,\tau(\nu, p_L, 0) - \int_{p_L}^{p_0} B[\nu, T(p)]\,\frac{d\tau(\nu, p, 0)}{dp}\,dp\right\} \tag{24}$$

or

$$I(\nu, 0) = I_{clr}(\nu, 0) - \beta X[\nu, p_U, p_L, T(p)] - a^* y[\nu, p_L, T(p)] \tag{25}$$

where the first two terms on the right hand side of eqn. (24) correspond to $I_{clr}(\nu, \theta)$ and

$$x[\nu, p_U, p_L, T(p)] = \left\{B[\nu, T(p_0)]\,\tau(\nu, p_0, 0) - B[\nu, T(p_U)]\,\tau(\nu, p_U, 0)\right.$$

$$\left.-\int_{p_U}^{p_0} B[\nu, T(p)]\,\frac{d\tau(\nu, p, 0)}{dp}\,dp\right\} \tag{26}$$

$$y\,[\nu, p_L, T\,(p)] = \left\{B\,[\nu, T(p_0)]\,\tau\,(\nu, p_0, \theta) - B\,[\nu, T(p_L)]\,\tau\,(\nu, p_L, 0)\right.$$

$$\left. - \int_{p_L}^{p_0} B\,[\nu, T\,(p)]\ \frac{d\tau\ (\nu, p, 0)}{dp}\ dp\right\} \tag{27}$$

and

$$a^* = a\,(1 - \beta). \tag{28}$$

Here subscripts U and L refer to upper and lower clouds. In case the clouds at one level are not randomly distributed with respect to clouds at the other level the above equation will still hold good but the physical significance of quantities a and β will be different. Rearranging eqn. (25) we get

$$I_{clr}\,(\nu, 0) = I\,(\nu, 0) + \beta x\,[\nu, p_U, p_L, T(p)] + a y\,[\nu, p_L, T(p)] \tag{29}$$

or

$$I_{clr}\,(\nu, 0) = I\,(\nu, 0) + c\,(\nu, 0) \tag{30}$$

where

$$c\,(\nu, 0) = \beta x\,[\nu, p_U, p_L, T(p)] + a^*\,y\,[\nu, p_L, T(p)] \tag{31}$$

is the correction that has to be added to the measured radiance to get $I_{clr}\,(\nu, \theta)$.

Now the problem is the estimation of most probable values of β, a^*, p_U and p_L to estimate the correction $c\,(\nu, 0)$. Since the first estimate of temperature profile could be obtained by six channel regression method discussed earlier, the estimation of I_{clr} $(\nu, 0)$ say $\tilde{I}_{clr}\,(\nu, 0)$ could be deduced for channels most sensitive to clouds, *viz.*, 714 cm^{-1}, 750 cm^{-1} and 899 cm^{-1}, using

$$\tilde{I}_{clr}\,(\nu, 0) = B\,[\nu, T(p_0)]\,\tau\,(\nu, p_0, 0) - \int_0^{p_0} B\,[\nu, T\,(p)]\,\frac{d\tau\,(\nu, p, \theta)}{dp}\,dp$$

for $y = 714$, 750 and 899 cm^{-1}.

and as $I\,(\nu, \theta)$ in these channels is known from measurements, first estimate of correction $\tilde{c}\,(\nu, \theta)$ could be made using eqn. (30) in the form

$$\tilde{c}\,(\nu, 0) = \tilde{I}_{clr}\,(\nu, 0) - I\,(\nu, \theta) \text{ for } \nu = 714, 750 \text{ and } 899\ cm^{-1}. \tag{32}$$

Now clouds are allowed to exist at any two-level combinations of standard pressure levels below 150 mb level, *viz.*, 200 mb, 250 mb, 300 mb, 400 mb, 500 mb, 700 mb. 850 mb and 1000 mb levels thinking that cloud tops do not generally cross 200 mb level. Now taking different two-level combinations and using 714 cm^{-1} (ν_1) and

899 cm^{-1} (ν_2) channels the eqn. (31), putting $\tilde{c}\,(\nu, 0)$ the estimate in place of $c\,(\nu, 0)$, could be written as

$$\tilde{c}\,(\nu_1, \theta) = \beta x'\,[\nu_1, p_U, p_L, T(p)] + a^*\,y'\,[\nu_1, p_L, T(p)] \text{ for } \nu_1 = 714 \text{ cm}^{-1} \tag{33}$$

$$\tilde{c}\,(\nu_2, 0) = \beta x''\,[\nu_2, p_U, p_L, T(p)] + a^*\,y''\,[\nu_2, p_L, T(p)] \text{ for } \nu_2 = 899 \text{ cm}^{-1} \tag{34}$$

Since we have assumed different two-level combinations for clouds and first approximation of temperature profile is known, x', x'', y' and y'' could be calculated using eqns. (26) and (27). As $\tilde{c}\,(\nu_1, 0)$ and $\tilde{c}\,(\nu_2, 0)$ would be available from eqn. (32), eqns. (33) and (34) containing only two unknowns β and a^* could be solved for those. Thus we get the values of β and a^* for different sets of two-level combinations. Here it may sometimes happen that values for these may turn out to be below zero or above unity but these are limited to zero and unity for obvious physical reasons.

To find out the most probable values of cloud parameters, namely, p_U, p_L, a^* and β, the value of $c\,(\nu_1, \theta)$ in 750 cm^{-1} channel is determined using eqn. (31) for different sets of values of β and a^* corresponding to different p_U and p_L combinations (first estimate of temperature profile required for such estimation is already available) while another value of $\tilde{c}\,(\nu, \theta)$ for $\nu = 750$ cm^{-1} channel is obtained using eqn. (32) and the most probable values of cloud characteristics are those set values which satisfy the criteria

$$|\,c\,(\nu, \theta) - \tilde{c}\,(\nu, \theta)\,| = \text{minimum for } \nu = 750 \text{ cm}^{-1}.$$

Now using these cloud characteristic parameters another estimates of $I_{clr}\,(\nu, \theta)$ are determined using eqn. (30) for those six channels which were used to determine the first estimate of temperature profile. These new determined values of $I_{clr}\,(\nu, \theta)$ for those six channels are again used to find out the second estimate of temperature profile using regression method. Again the whole process is repeated and this is done till the cloud correction $[c\,(\nu, \theta)]$ ceases to change. After this the value of $I_{clr}\,(\nu, \theta)$ is calculated for all the eight channels and by using regression method most probable temperature profile is obtained. Since the actual radiances received in the presence of clouds will be less than what those would have been in the absence of clouds, the first estimate of temperature profile will be colder than the true profile and in each iteration step it will improve. It is experienced that normally four iteration steps bring the convergence in the cloud correction and consequently in the temperature profile.

(*d*) *Multiple field of view approach*

The clouds are nearly opaque to infrared region radiations and thus very little radiance arising below cloud levels will be allowed to pass through the clouds resulting in very

little impressions about the temperature structure below cloud level in the observed radiances. Secondly the observed radiances could arise due to various combination of cloud and temperature structures and thus the range of valid solutions for temperature profile for a given set of radiances becomes wide. In multiple field of view approach an attempt to modify these limitations of single field of view approach is made. Multiple field of view approach using high spatial resolution scanning radiometer is based on the reasoning that the scale of horizontal variability of temperature profile is much larger than the scale of horizontal variability of clouds. In other words if we take contiguous measurements of radiance then it is possible to assume safely that cloud characteristics such as transmissivity, emissivity, reflectivity and the atmospheric clear column radiance do not vary much while cloud amount will vary significantly. Thus this approach is valid only when the variation in radiances arises due to the variation in cloud amount which in turn demands higher spatial resolution. Using eqn. (13) and applying above cited approximations the radiance observed in a channel corresponding to wave number v for two nearly contiguous fields of view could be written as

$$I_1(v, 0) = N_1 I_{cd}(v, 0) + (1 - N_1) I_{clr}(v, 0) \tag{35}$$

$$I_2(v, 0) = N_2 I_{cd}(v, 0) + (1 - N_2) I_{clr}(v, 0) \tag{36}$$

where $I_1(v, 0)$ and $I_2(v, 0)$ refer to the amount of radiance observed in the first and second fields of view respectively while N_1 and N_2 correspond to the amount of clouds in the first and second fields of view respectively. Multiplying eqn. (35) by N_2 and eqn. (36) by N_1 and subtracting (36) from (35) to eliminate $I_{cd}(v, \theta)$ we get

$$I_{clr}(v, 0)(N_2 - N_1) = I_1(v, 0) N_2 - I_2(v, 0) N_1$$

On dividing both the sides by N_2 and putting

$$N^* = \frac{N_1}{N_2}, \text{ we get}$$

$$I_{clr}(v, 0) = \frac{I_1(v, 0) - N^* I_2(v, 0)}{1 - N^*} \tag{37}$$

Equation (37) shows that $I_{clr}(v, 0)$ could be calculated provided N^* is known. Now evaluation of N^* could be done using window channel ($v = \omega$) data in both the fields of view for which case eqn. (37) becomes

$$I_{clr}(\omega, 0) = \frac{I_1(\omega, 0) - N^* I_2(\omega, 0)}{1 - N^*} \tag{38}$$

where $I_1(\omega, 0)$ and $I_2(\omega, 0)$ correspond to radiances in the window channel from the first and second fields of view respectively. $I_{clr}(\omega, 0)$ will be given by

$$I_{clr}(\omega, \theta) = B[\omega, T(p_0)]\, \tau(\omega, p_0, \theta) - \int_0^{p_0} B[\omega, T(p)] \frac{d\tau(\omega, p, \theta)}{dp}\, dp \tag{39}$$

In the above equation which is for window channel the second term on the right hand side could be considered zero as in the window channel there will be negligible atmospheric contribution to the observed radiance while the transmittance function $\tau(\omega, p_0, \theta)$ could be considered equal to unity as there will be little absorption by the atmosphere in the window channel. Thus the eqn. (39) reduces to

$$I_{clr}(\omega, \theta) = B[\omega, T(p_0)]$$

where p_0 refers to surface pressure. Substituting for $I_{clr}(\omega, \theta)$ in eqn. (38) we get

$$N^* = \frac{I_1(\omega, \theta) - B[\omega, T(p_0)]}{I_2(\omega, \theta) - B[\omega, T(p_0)]}. \tag{40}$$

Determination of N^* needs the value of surface temperature which could be determined using radiance data in two window channels ω_1 (3·7 μm) and ω_2 (11 μm). Writing expression for N^* for window channels ω_1 and ω_2 we get [from eqn. (40)]

$$N^* = \frac{I_1(\omega_1, \theta) - B[\omega_1, T(p_0)]}{I_2(\omega_1, \theta) - B[\omega_1, T(p_0)]} \tag{41}$$

and

$$N^* = \frac{I_1(\omega_2, \theta) - B[\omega_2, T(p_0)]}{I_2(\omega_2, \theta) - B[\omega_2, T(p_0)]} \tag{42}$$

Eliminating N^* from eqns. (41) and (42) we get

$$\begin{aligned} &\{I_1(\omega_1, \theta)\, I_2(\omega_2, \theta) - I_1(\omega_2, \theta)\, I_2(\omega_1, \theta)\} \\ &+ B[\omega_2, T(p_0)]\, \{I_2(\omega_1, \theta) - I_1(\omega_1, \theta)\} \\ &- B[\omega_1, T(p_0)]\, \{I_2(\omega_2, \theta) - I_1(\omega_2, \theta)\} = 0. \end{aligned} \tag{43}$$

Now the surface temperature could be obtained from eqn. (43) as only $T(p_0)$ is the unknown quantity in this equation. Once $T(p_0)$ is determined N^* could be determined using eqn. (40) and on knowing N^*, $I_{clr}(\nu, 0)$ could be made known by using eqn. (37). After finding out $I_{clr}(\nu, 0)$ for all the eight channels by this method the temperature profile could be estimated using regression method.

Chahine[41] has developed analytical method, for a single cloud layer, for constructing the clear column temperature profile from the apparent temperature profile derived without accounting the effects of clouds in the measured radiances. Analytical transformation formulae developed, under single field of view approach, for getting tempe-

rature profiles below cloud top level and above cloud level with a discontinuity for temperature information at the cloud top pressure (p_c) level involves the knowledge of cloud amount and p_c value. The evaluation of p_c is more difficult when it lies in between two sounding levels. In the two fields of view approach the developed transformation formula does not involve p_c explicitly. These analytical methods have been backed only by numerical methods. Now the question is when tc apply correction for the presence of clouds in the field of view. When the brightness temperature derived from window channel radiance measurements is less then 5° K or more from the prespecified surface temperature (could be climatic value) it is understood that clouds are present in the field of view and then one of the above discussed methods is used to find out $I_{clr}(\nu, \theta)$ and ultimately the temperature profile using regression method. This criteria of identifying the cloudy regions from infrared radiance data could be useful in cases of generally broken or overcast middle or high cloudiness but in cases of widely scattered small clouds, very thin cirrus, very low cloud layers or fog, this criteria may not be able to detect cloud presence as the IR radiance will only be slightly lowered. Due to much reflectivity of visible light from low clouds and fogs as compared to that for sea surface, use of coincident visible data will be able to tell about the presence of clouds. However the detection of thin cirrus and widely scattered small clouds is a very difficult problem.

4. Corrections due to high terrain and hot terrain

Corrections due to high terrain, *i.e.*, terrain at 400 meters and above mean sea level which causes significant radiative departures from mean sea level conditions could be estimated considering terrain as the lower cloud level and clouds in a single cloud layer as second level in two-level cloud model. It may sometimes happen that ground is much warmer than the air layer just above it due to bad thermal conductivity of the air. In such cases when the ground temperature (T_g) derived from the brightness temperature calculations in window channel exceeds the conventional surface temperature (T_{sh}) by 5° K or more, correction due to hot terrain has to be applied, *i.e.*, instead of having ground as the lower boundary in the observed radiance we have to have the lower boundary corresponding to temperature T_{sh}. So we have to subtract from the observed radiance the radiative contribution from the ground boundary and to add the radiance contribution from air layer corresponding to temperature T_{sh}. Thus the expression for the correction due to hot terrain for each channel will be

$$k(\nu, \theta) = \{B(\nu, T_{sh}) - B(\nu, T_g)\}\, \tau\ (\nu, p_0, \theta)$$

and this has to be added to the observed radiance to account for the error that arises due to hot terrain. A detailed account of application of these appears in Smith *et al.*[40]

5. Effect of absorption by water vapour in 15 μm band

Though the temperature retrieval by regression method would not be seriously affected by water vapour absorption in the 15 μm CO_2 band yet it is discussed to bring out the limi-

tation aspect of 15 μm band in estimating temperature below 700 mb level. Unlike cloud-free environment case the regression method in the presence of clouds, especially in single field of view approach, involves physical quantities such as gas transmittances and therefore it is worth to discuss the water vapour absorption effect in 15 μm band. Weinreb[42] has simulated the effect of overlapping water vapour continuum and spectral lines on the weighting functions corresponding to 725 cm^{-1} and 747 cm^{-1} channels of Vertical Temperature Profile Radiometer (McMillan *et al.*[43], Wark *et al.*[44]) and studied the variation in temperature profile, retrieved through minimum information method (Fleming and Smith[45]) with changes in water vapour mixing ratio. The increase in water vapour raises the weighting function in the atmosphere. Minimum information method using forecast profile as initial value is expected to have 1–3°C rms error chiefly due to fundamental difficulties in solving the encountered Fredholm equation (Philips[46]). Considering the retrieved profile valid till rms error of retrieved temperatures does not exceed rms the error of initial forecast temperatures, Weinreb[42] has shown that over 0–20° N latitude retrieved profile below 700 mb will be much affected once ρ (rms per cent error in mixing ratio introduced during simulation) $> 20\%$ while in case of 50–60° N latitude this will happen when $\rho > 35\%$. Obviously rms error of retrieved temperature increases with the increase in ρ and in 0–20° N latitude the altitude up to which this error effects considerably shifts downward with increasing ρ and is confined to below 850 mb for $\rho > 60\%$.

6. Effect of aerosols

There are basic difficulties while dealing with aerosols contribution to the observed radiances due to

(1) Lack of understanding of the heat exchange mechanism between the particle and its surroundings and in the absence of such knowledge one has only to assume the prevalence of local thermodynamic equilibrium.

(2) Lack of understanding about the shape, scattering, and absorption characteristics of aerosols. The aerosols scatter radiations in an asymmetric fashion and a complete description of radiation field interaction with atmospheric layer containing aerosols will demand for the degree and direction of polarization, ellipticity of radiation and phase functions of aerosols. Under the circumstances the assumption of spherical shape of aerosols coated with a thick water layer is made, to use Mie scattering theory which could lead to a highly polarized thermal emission under hazy conditions. But in the case of terrestrial unpolarized infrared radiations the contribution due to scattering will be small enough to render the effect of polarization unimportant.

(3) High variability of aerosol size distribution, concentrations, and the variability in the optical nature of aerosols.

Stowe[47, 48] has carried out investigation for the effect of particulate matter on the radiance of terrestrial infrared radiations using Rossen[49] and Elterman[50] vertical distri-

bution of aerosols and corresponding temperature profile, and Diermendjian[51] computations on the size distribution of aerosols. He has computed the change in the terrestrial radiation due to emission from aerosols as a fraction of clear atmospheric radiance (E), contribution of scattering by taking ratio of radiance due to scattering and that due to non-turbid clear atmosphere (S), and the change in the total radiance (both emission and scattering) due to aerosols as a fraction of non-turbid clear atmosphere (R). In general he has found that $E < 0, S < |E|, R < 0$ and the terrestrial radiations in the 15 μm band do not get altered by more than 1% due to the presence of aerosols. Due to large atmospheric attenuation of radiations emitted in lower levels the emission in the centre of an absorption band arises mainly from higher levels where the effect of aerosols is generally less because of low aerosol concentration and short optical path traversed. In the case of emission in the wings of an absorption band, which arises from lower levels, the contribution of aerosols to the observed radiance will be comparatively more due to increased optical path traversed and high concentration of aerosols in the lower atmospheric regions. Aerosols in addition to effecting the radiance received at satellite will also modify the transmittance and weighting functions. Stowe[47] believes that combination of all these effects will result in significantly modifying the temperature profile derived from satellite radiance measurements and the effect of aerosols will obviously be much reflected in those atmospheric regions where aerosol concentrations are high. It may be worth to add here that recently Toon and Pollack[52] have designed a model of size distribution, chemical composition and optical thickness of stratospheric and tropospheric aerosols for the purpose of global average radiative transfer calculations.

7. Microwave technique

Though the microwave technique exploiting microwave spin rotational band of oxygen arising due to magnetic dipole transitions near 60 GHz and single transition near 118 GHz are not still in operational use. yet it becomes obligatory to deal with it as this provides an opportunity to determine the temperature profile under complete overcast conditions which has not been possible using infrared temperature measurements. Using microwave techniques it is possible to get the temperature profile from altitude 20 to 130 km. Water *et al.*[53, 54] have discussed microwave temperature measurements in two weak water vapour resonance channels centering at 22·235 and 31·4 GHz (1 cm spectral window band) and three oxygen channels centering at 53·65, 54·9 and 58·8 GHz (5 mm strong O_2 resonance band) using Nimbus E microwave spectrometer (NEMS) observations. The 5-mm band channels are primarily for atmospheric temperature profile while the 1-cm band channels indicate land emissivity and temperature and are sensitive to water vapour and liquid water over oceans. In microwave measurements the lower boundary (Earth's surface) contribution has to be multiplied by emissivity unlike in infrared measurements where lower boundary is considered as black body while the atmosphere is considered nearly opaque for radiative energy components received in oxygen band. The weighting functions for oxygen

channels at 53·65, 54·9 and 58·8 GHz which peak nearly at 4, 11 and 18 km altitudes are considered to be weakly dependent on temperature profile, atmospheric water content and surface-reflectivity. The half width of weighting functions is from 8 to 12 km. Waters *et al.*[53, 54] compared NEMS derived temperature profiles with NMC (National Meteorological Center, U.S.A.). Northern Hemispheric Analysis grid data which were arrived at using radiosonde data, commercial aircraft flight data and Vertical Temperature Profile Radiometer (NOAA 2) data (for coverage over ocean areas). They found that features of warm lower stratosphere and extremely cold lower troposphere for January 18, 1973 (1941 GMT) Poker Flats (Alaska) flight and very cold tropopause and warm lower troposphere for June 27, 1975 (1615 GMT) Ft. Sherman (Panama) flight were not reproduced by NEMS measurements. These two flights were chosen as they contained extremes of surface temperatures out of the 82 coincident flights examined by them. They have further illustrated that features of small vertical extent, *e.g.*, narrow cold features, sharp inversions could not be reproduced by NEMS measurements. Out of the three temperature profile producing oxygen channels, the 53·65 GHz channel is the deep penetrating channel and is considerably affected by clouds as the very thick clouds at great altitudes will have considerable affect on 53·75 GHz channel measurements because the clouds will normally be colder than the brightness temperature (equivalent black body temperature which could radiate power equal to the observed microwave signal intensity) corresponding to the radiations incident on cloud from below. Since the channels 54·9 and 58·8 GHz have their weighting functions peaking at 11 and 18 km respectively these are less affected by the presence of heavy clouds. Presence of cirrus clouds cause negligible effect because they are thin and have very low microwave absorption characteristics. Staelin[55] has discussed the effect of clouds on NEMS temperature soundings. As the microwave absorption for the oxygen band in case of cloud of non-precipitative characteristics (drop diameter $\lesssim 100\,\mu$m) is given by

$$3{\cdot}55 \times 10^{-3-(T/82)}\, M\lambda^{-2}\ (\mathrm{cm}^{-1})$$

where

M stands for liquid water density of cloud in g/m^3,

λ stands for wavelength in cm, and

T for cloud temperature in Kelvin,

the clouds with water content $<$ ·01 gm/cm^2 will not be seriously affecting the temperature profile. However heavy clouds with water content say 0·1 gm/cm^2 may cause sufficient errors in temperature measurements.

Staelin *et al.* have found that presence of attenuating portions of clouds below near about 4 km altitude or their distribution in small isolated cells over wide area could cause an error of 1° K in temperature measurements in 53·65 GHz channel while in cases of extension of large attenuating portions above 4 km altitude or their being in

tightly packed cells clustering over an area comparable to the field of view of spectrometer (200 km in NEMS) the error could be of 5 to 10° K. As the instrument gets the averaged radiance over the field of view of 200 km it is obvious to have more error if the error producing heavy clouds are present in tightly packed cells over an extended area. The 31·4 GHz (9 mm) channel as compared to 22·235 GHz (13 mm) channel over the ocean is 0·4 times sensitive to water vapour while it is two times sensitive to cloud which results in accurate estimation of clouds and water vapour with accuracies of 0·04 gm/cm² and 0·1 gm/cm² respectively enabling separate estimation of water vapour and clouds using both the channels. Errors in this estimation could result from much sea foam and reflection of sunlight near the equator at noon. Using these two channels surface temperature over land could be estimated for regions where surface emissivity is known either by comparison of microwave and direct measurements or by its estimation based on known surface temperature.

The variation in brightness temperature could arise due to variations in atmospheric temperatures, surface temperatures and due to the presence of heavy clouds. Staelin *et al.* studied the sensitivity of 53·65 GHz channel over the near equatorial traverses at equator crossing longitudes of 13·5° W, 126·2° E, 72·5° E, 94·1° W, 153·0° E and 40·5° W on December 23, 1972, choice for equatorial traverses was based on the consideration of minimum atmospheric temperature variations. They observed abrupt increase of ~ 1·5° K in brightness temperature during passes from ocean to Mexican coast near Acapulco, from ocean to the coast of Australia, and near the equator over the tip of Brazil. Such an abrupt increase in brightness temperature during transitions from ocean to land occurs due to increase in emissivity from 0·5 in ocean to 0·8–1·0 over land. This effect could be compensated using surface emissivity information available in radiances observed in 22·235 and 31·4 GHz channels. They observed that brightness temperatures derived in the absence of sea-land transitions and heavy clouds were stable and unperturbed even in the presence of a wide variety of ordinary clouds. They have further concluded that in the absence of clouds small temperature gradients could be observed with an accuracy of few tenths of a degree Kelvin over distances of hundreds to thousands of kilometers.

8. Acknowledgement

The author is indebted to Dr. K. R. Saha for initiating and actuating him to this field and for his perceptive guidance and inspiring comments. Thanks are due to Shri Brij Mohan for his unique assistance in manuscript preparation, to Shri M. H. Gangawane for his diligence and lively efficiency in typing the manuscript. The author is profoundly grateful to the Director, Indian Institute of Tropical Meteorology, Pune, for permitting the publication of this manuscript.

References

1. Kaplan, L. D. Inference of atmospheric structure from remote radiation measurements, *J. Optical Socy. Amer.*, 1959, 49, 1004–1007.

2. RODGERS, C. D. — Retrieval of atmospheric temperature and composition from remote measurements of thermal radiation, *Revs. Geophys. and Space Phys.*, 1976, **14**, 609–624.

3. HOUGHTON, J. T. AND SMITH, S. D. — The selective chopper radiometer (SCR) experiment, *The NIMBUS 5 User's Guide*, Goddard Space Flight Center, Greenbelt, Maryland, 1972, pp. 131–140.

4. BARNETT, J. J., CROSS, M. J., HARWOOD, R. S., HOUGHTON, J. T., MORGAN, C. G., PECKHAM, G. E., RODGERS, C. D., SMITH, S. D. AND WILLIAMSON, E. J. — The first year of the selective chopper radiometer on NIMBUS 4, *Quart. J. Royal Meteorol. Socy.*, 1972, **98**, 17–37.

5. ELLIS, P., HOLAH, G., HOUGHTON, J. T., JONES, T. S., PECKHAM, G. E., PESKETT, G. D., PICK, D. R., RODGERS, C. D., ROSCOE, H., SANDWELL, R., SMITH, S. D. AND WILLIAMSON, E. J. — Remote sounding of atmospheric temperature from satellites IV. The selective chopper radiometer for NIMBUS 5, *Proc. Royal Socy., London*, 1973, A **334** (1597), 149–170.

6. HOUGHTON, J. T, — The pressure modulator radiometer (PMR) experiment, *The NIMBUS 6 User's Guide*, Goddard Space Flight Center, Greenbelt, Maryland, 1975, pp. 163–171.

7. CURTIS, P. D., HOUGHTON, J. T., PESKETT, G. D. AND RODGERS, C. D. — Remote sounding of atmospheric temperature from satellites. V. The pressure modulated radiometer for Nimbus F, *Proc. Royal Socy. London*, 1974, A **337** (1608), 135–150.

8. GILLE, J. C., HOUSE, F. B., CRAIG, R. A. AND THOMAS, J. R. — The limb radiance inversion radiometer (LRIR) experiment, *The NIMBUS 6 User's Guide*, Goddard Space Flight Center, Greenbelt, Maryland, 1975, pp. 141–161.

9. GILLE, J. C. — Limb radiance inversion techniques, *Proc. of the Society of Photo-optical Instrumentation Engineers*, Scanners and Imagery Systems for Earth observations, 1975, **51**, 15–20.

10. RODGERS, C. D. — The Nimbus G limb-scanning pressure modulated radiometer, Proc. of a workshop held at National Center for Atmospheric Research, 14–18 July, 1975, *The Stratosphere and Mesosphere: Dynamics, Physics and Chemistry*, Satellite Workshop, NCAR/CQ-4 + 1975-ASP, 1975, **2**, 120–123.

11. RUSSELL, J. — The Nimbus G limb-scanning radiometer LIMS (Limb Infrared Monitor of the Stratosphere), 1975, *Ibid.*, pp. 112–119.

12. COURANT, R. AND HILBERT, D. — *Methods of Mathematical Physics*, Interscience Publishers, New York, 1953, **1**, 561 pp.

13. RODGERS, C. D. — The vertical resolution of remotely sounded temperature profiles with *a priori* statistics, *J. Atmos. Sci.*, 1976, **33**, 707–709.

14. BACKUS, G. E. AND GILBERT, J. F. Uniqueness in the inversion of inaccurate gross earth data, *Phil. Trans. Royal Socy., London*, 1970, A 266, 123–192.

15. CONRATH, B. J. Vertical resolution of temperature profiles obtained from remote radiation measurements, *J. Atmos. Sci.*, 1972, 29, 1262–1271.

16. FRITZ, S., WARK, D. Q., FLEMING, H. E., SMITH, W. L., JACOBITZ, H., HILLEARY, D. T. AND ALIHOUSE, J. C. Temperature sounding from satellites, *NOAA TR NESS* 59, National Oceanic and Atmospheric Administration, Washington D.C., 1972, p. 49.

17. MILLER, G. F. Fredholm equations of the first kind, In *Numerical Solution of Integral Equations*, edited by L. M. Delvas and J. Walsch, Clarendon Press, Oxford, 1974.

18. TWOMEY, S. The application of numerical filtering to the solution of integral equations encountered in indirect sensing measurements, *J. Franklin Institute*, 1965, 279, 95–109.

19. STRAND, O. N. AND WESTWATER, ED. R. Statistical estimation of the numerical solution of a Fredholm integral equation of the first kind, *J. Association of Computing Machinery*, 1968, 15, 100–114.

20. STRAND, O N. AND WESTWATER, ED. R. Minimum-RMS estimation of the numerical solution of a Fredholm integral equation of the first kind, *SIAM J. Numerical Analysis*, 1968, 5, 287–295.

21. WESTWATER, ED. R. AND STRAND, O. N. Inversion Techniques, In *Remote Sensing of the Troposphere*, edited by V. E. Derr, Chapter 16, National Oceanic and Atmospheric Administration, Washington, D.C., 1972.

22. WAHBA, G. On the numerical solution of Fredholm integral equation of the first kind, *Technical Report No.* 217, Department of Statistics, University of Wisconsin, Madison, Wisconsin, 1969, p. 60.

23. STRAND, O. N. Theory and methods related to the singular function expansion and Landweber's iteration for the integral equations of the first kind, *SIAM J. Numerical Analysis*, 1974, 11, 798–825.

24. COLIN, L. Mathematics of profile inversion, *Proc. of a workshop held at NASA Ames Research Center*, Moffett Field, California, July 12–16, 1971, NASA TM X-62, 1972, 150.

25. JASTROW, R. AND HALEM, M. Accuracy and coverage of temperature data derived from the IR radiometer on NOAA 2 satellite, *J. Atmos. Sci.*, 1973, 30, 958–964.

26. WARK, D. Q. Atmospheric transmittance used in indirect soundings of the earth's atmosphere, paper presented at the International Radiation Symposium, International Association of Atmospheric Physics, World Meteorol. Org.: International Council of Scientific Unions, Amer. Meteorol. Socy. and Meteorol. Socy. of Japan, Sendai, Japan, May 26–June 2, 1972.

27. WEINREB, M. P. AND FLEMING, H. E. Empirical radiance corrections: a technique to improve satellite soundings of atmospheric temperature, *Geophys. Res. Letters*, 1974, 1, 298–301.

28. FLEMING, H. E. — Improving the vertical resolution of satellite temperature retrieval by channel differencing, *Symposium on Remote Sensing*, Nov. 16–19, 1976, Melbourne.

29. PRABHAKARA. C., RODGERS, E. B., CONRATH, B. J., HANEL, R. A. AND KUNDE, V. G. — The Nimbus 4 infrared spectroscopy experiment 3. Observations of the lower stratospheric thermal structure and total ozone, *J. Geophys. Res.*, 1976, **81**, 6391–6399.

30. HORN, L. H., PETERSON, R. A. AND WHITTAKER, T. A. — Intercomparisons of data retrieved from Nimbus 5 temperature profiles, rawinsonde observations and initialized LFM model fields, *Mon. Wea. Rev.*, 1976, **104**, 1362–1371.

31. — Global Atmospheric Research Program, *Publication Ser. No.* 11, *The First GARP Global Experiment, Objectives and Plans*, Chapter 5: Observational requirements for the experiment, World Meteorological Organisation, 1973.

32. GANDIN, L. S. — Objective analysis of meteorological fields, 1963, *Gidrometeor. Izd.*, 242 pp. (Translated by Israel Program for Scientific Translations, Jerusalem, 1965).

33. ALAKA, M. A. AND ELVANDER, R. C. — Optimum interpolation from observations of mixed quality, *Mon. Wea. Rev.*, 1972, **100**, 612–624.

34. ALAKA, M. A. AND ELVANDER, R. C. — Matching of observational accuracy and sampling reduction in meteorological data acquisition experiments, *J. Appl. Meteorol.*, 1972, **11**, 567–577.

35. BERGMAN, K. H. AND BONNER, W. D. — Analysis error as a function of observational density for satellite temperature soundings with spatially correlated errors, *Mon. Wea. Rev.*, 1976, **104**, 1308–1316.

36. BENGTSSON, L. AND GUSTAVSSON, N. — An experiment in the assimilation of data in dynamical analysis, *Tellus*, 1971, **23**, 328–336.

37. GANDIN, L. S., KAGAN, R. S. AND POLISHCHUK, A. I. — Estimation of the information content of meteorological observing systems, *Leningrad Gl. Geofiz. Observ.*, 1972, Trudy No. 286, pp. 120–140.

38. BERGMAN, K. H. AND BONNER, W. D. — Addendum to analysis error as a function of observation density for satellite temperature soundings with spatially correlated errors, *Mon. Wea. Rev.*, 1977, **105**, 549.

39. KUHN, P. M., WEICKMANN, H. K., LOJKO, M. J. AND STEARNS, L. P. — Transfer of infrared radiation through clouds, *Applied Optics*, 1974, **13**, 512–517.

40. SMITH, W. L., WOOLF, H. M. AND FLEMING, H. E. — Retrieval of atmospheric temperature profiles from satellite measurements for dynamical forecasting, *J. Appl. Meteorol.*, 1972, **11**, 113–122.

41. CHAHINE, M. T. — An analytical transformation for remote sensing of clear-column atmospheric temperature profiles, *J. Atmos. Sci.*, 1975, **32**, 1946–1952.

42. WEINREB, M. P. — Sensitivity of satellite retrievals of temperature to errors in estimates of tropospheric water vapour, *J. Appl. Meteorol.*, 1977, **16**, 605–613.

43. MCMILLIN, L. M., WARK, D. Q., SIOMKAJLO, J. M., ABEL, P. G., WERBOWETZKI, A., LAURITSON, L. A., PRITCHARD, J. A., CROSBY, D. S., WOOLF, H. M., LUEBBE, R. C., WEINREB, M. P., FLEMING, H. E., BITTNER, F. E. AND HAYDEN, C. M. — Satellite infrared soundings from NOAA spacecraft, *NOAA Tech. Rep. NESS* 65, National Environmental Satellite Service, Washington, D.C., 1973, pp. 112.

44 WARK, D. Q., LIENESCH, J. H. AND WEINREB, M. P. — Satellite observations of atmospheric water vapour, *Appl. Opt.*, 1974, **13**, 507–511.

45. FLEMING, H. E. AND SMITH, W. L. — Inversion techniques for remote sensing of atmospheric temperature profiles, In *Temperature : its measurements and control in Science and Industry*, edited by H. H. Plumb, Instrum. Socy. Amer., 1972, **4**, 2239–2250.

46. PHILLIPS, D. L. — A technique for the numerical solution of certain integral equations of the first kind, *J. Assoc. Comp. Mach.*, 1962, **9**, 84–97.

47. STOWE, L. L., JR. — The effects of particulate matter on the radiance of terrestrial infrared radiation, *Research Report*, Institute of Geophysics and Planetary Physics, University of California, Los Angeles, California, 1971, pp 109.

48. STOWE, L. L. JR. — Effects of particulate matter on the radiance of terrestrial infrared radiation : Results, *J. Atmos. Sci.*, 1973, **31**, 755–767.

49. ROSSEN, J. M. — Simultaneous dust and ozone soundings over North and Central America, *Atmospheric Physics*–25, Report N 68–11414, University of Minnesota.

50. ELTERMANN, L. — Aerosol measurements in the troposphere and stratosphere, *Applied Optics*, 1966, **5**, 1769–1776.

51. DIERMENDJIAN, D. — *Electromagnetic Scattering on Spherical Polydispersion*, American Elsevier Publishing Company Inc., New York, 1969, p. 290.

52. TOON, O. B. AND POLLACK, J. B. — A global average model of atmospheric aerosols for radiative transfer calculations, *J. Appl. Meteorol.*, 1976, **15**, 225–246.

53. WATERS, J. M., STAELIN, D. H., KUNZI, K. F., PETTYJOHN, R. L. AND POON, P. K. L. — Microwave remote sensing of atmospheric temperatures from the Nimbus 5 satellite, *Space Research*, Akademie-Verlag, Berlin, 1975, p. 117.

54. WATERS, J. M., KUNZI, K. F., PETTYJOHN, R. L., POON, P. K. L. AND STAELIN, D. H. Remote sensing of atmospheric temperature profiles with the Nimbus 5 microwave spectrometer, *J. Atmos. Sci.*, 1975, **32**, 1953–1969.

55. STAELIN, D. H., CASSEL, A. L., KUNZI, K. F., PETTYJOHN, R. L., POON, P. K. L., ROSENKRANZ, P. W. AND WATERS, J. M. Microwave atmospheric temperature sounding: effects of cloud on the Nimbus 5 satellite data, *J. Atmos. Sci.*, 1975, **32**, 1970–1976.